Beams-doc-1893-v3
July 28, 2005

Third Order Calculation of Beam Position

Rob Kutschke, CD/EXP

Abstract

This note works out the third order estimate for the beam position, for use with the upgraded Tevatron BPMs, including corrections for the unmeasured coordinate. The note includes figures that illustrate the residual error that remains after the corrections are made. Code to implement the correction has been placed in the DocDB along with this writeup. The main result of the paper is in Figure 5, which shows the accuracy that can be achieved online and Figure 6, which shows the accuracy that can be achieved offline. There is one important caveat: the treatment of the coupling between the electrodes may not be complete. An attempt to test this by comparing the sizes of the proton and anti-proton helices was not precise enough to be definitive. A further test is suggested.

1 Caveat

This note does not do a complete treatment of the coupling between the electrodes in the pickup. Hopefully a more complete treatment will only change the details, not the big picture.

2 Model Without Coupling

In Beams-doc-1161-v1, equation 6 gives the magnitudes of the A and B signals on a pickup as a function of beam position and current. The model ignores the coupling between the electrodes and any edge effects coming from the finite length of the electrodes. The model is,

$$A_0 = \frac{I_A}{I_{\rm beam}} = \frac{\phi}{2\pi}\left(1+\sum_{n=1}^{\infty}\frac{4}{n\phi}\left(\frac{r}{b}\right)^n \cos\left(n\theta\right)\sin\left(n\frac{\phi}{2}\right)\right) \quad (1)$$

$$B_0 = \frac{I_B}{I_{\rm beam}} = \frac{\phi}{2\pi}\left(1+\sum_{n=1}^{\infty}\frac{4}{n\phi}\left(\frac{r}{b}\right)^n \cos\left(n\theta\right)\sin\left(n(\pi+\frac{\phi}{2})\right)\right), \quad (2)$$

where the actual beam position is given in 2D polar coordinates (r,θ), where b is the radius of curvature of the electrodes and where the electrodes subtend an arc of angle ϕ. The origin of the coordinate system has been chosen so that x is the coordinate measured by the BPM while y is the orthogonal coordinate.

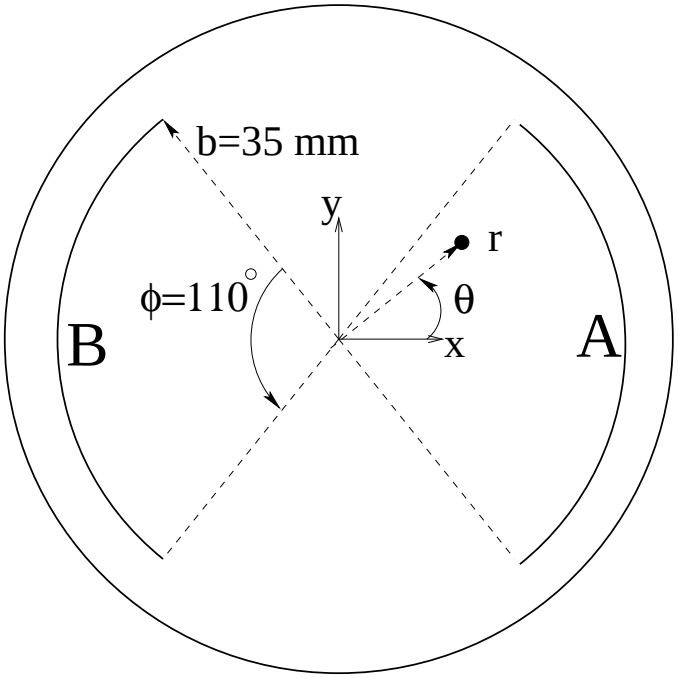

Figure 1: Definition of the parameters used in the equations. The two electrodes are labeled A and B. The electrodes are concentric arcs of a circle of radius b. The angle subtended by each electrode is given by ϕ. The BPM measures the x coordinate. The beam position is indicated by the filled dot and its position is denoted by either (x, y) or (r, θ). The numerical values come from Beams-doc-809.

These quantities are illustrated in Figure 1. The subscript 0 on A_0 and B_0 indicates that these quantities ignore coupling.

Expanding these equations to third order in r/b gives,

$$\begin{aligned} A_0 &= \frac{\phi}{2\pi}\left(1+\frac{4}{\phi}\frac{r}{b}\cos\theta\sin(\frac{\phi}{2})+\frac{4}{2\phi}\left(\frac{r}{b}\right)^2\cos(2\theta)\sin(\phi)\right. \\ &\quad \left.+\frac{4}{3\phi}\left(\frac{r}{b}\right)^3\cos(3\theta)\sin(\frac{3\phi}{2})+\ldots\right) \qquad (3) \\ B_0 &= \frac{\phi}{2\pi}\left(1+\frac{4}{\phi}\frac{r}{b}\cos\theta\sin(\pi+\frac{\phi}{2})+\frac{4}{2\phi}\left(\frac{r}{b}\right)^2\cos(2\theta)\sin(2(\pi+\frac{\phi}{2}))\right. \\ &\quad \left.+\frac{4}{3\phi}\left(\frac{r}{b}\right)^3\cos(3\theta)\sin(3(\pi+\frac{\phi}{2}))+\ldots\right) \qquad (4) \\ &= \frac{\phi}{2\pi}\left(1-\frac{4}{\phi}\frac{r}{b}\cos\theta\sin(\frac{\phi}{2})+\frac{4}{2\phi}\left(\frac{r}{b}\right)^2\cos(2\theta)\sin(\phi)\right. \end{aligned}$$

$$-\frac{4}{3\phi}\left(\frac{r}{b}\right)^3 \cos(3\theta)\sin(\frac{3\phi}{2}) + \ldots\Big) \tag{5}$$

In the last line, the only change is to reduce the $\sin\phi$ terms. These equations can be changed to Cartesian coordinates using,

$$\begin{aligned}
\cos(2\theta) &= \cos^2\theta - \sin^2\theta && (6)\\
\cos(3\theta) &= \cos(2\theta+\theta) && (7)\\
&= \cos(2\theta)\cos(\theta) - \sin(2\theta)\sin(\theta) && (8)\\
&= \left(\cos^2\theta - \sin^2\theta\right)\cos\theta - 2\sin\theta\cos\theta\sin\theta && (9)\\
&= \cos\theta\left(\cos^2\theta - 3\sin^2\theta\right). && (10)
\end{aligned}$$

This gives,

$$\begin{aligned}
A_0 &= \frac{\phi}{2\pi}\left(1 + a_1 x + a_2(x^2-y^2) + a_3 x(x^2-3y^2)\right) && (11)\\
B_0 &= \frac{\phi}{2\pi}\left(1 - a_1 x + a_2(x^2-y^2) - a_3 x(x^2-3y^2)\right), && (12)
\end{aligned}$$

where,

$$\begin{aligned}
a_1 &= \frac{4}{\phi\, b}\sin(\frac{\phi}{2}) && (13)\\
a_2 &= \frac{2}{\phi\, b^2}\sin(\phi) && (14)\\
a_3 &= \frac{4}{3\phi\, b^3}\sin(\frac{3\phi}{2}). && (15)
\end{aligned}$$

3 Adding Linear Coupling

If the electrodes A and B are linearly coupled, then the signals on A and B are given by,

$$\begin{aligned}
A &= A_0 + CB && (16)\\
B &= B_0 + CA, && (17)
\end{aligned}$$

where A and B are the signals including coupling and where C is the coupling coefficient. A_0 and B_0, the signals in the no-coupling limit, are given by equations 11 and 12, respectively. The solution to these equations is,

$$\begin{aligned}
A &= \frac{A_0 + CB_0}{1-C^2} && (18)\\
B &= \frac{B_0 + CA_0}{1-C^2} && (19)
\end{aligned}$$

Expanding to third order in r/b gives,

$$\begin{aligned}
A &= \frac{\phi}{2\pi}\frac{1}{1-C}\left(1 + b_1 x + b_2(x^2-y^2) + b_3 x(x^2-3y^2)\right) && (20)\\
B &= \frac{\phi}{2\pi}\frac{1}{1-C}\left(1 - b_1 x + b_2(x^2-y^2) - b_3 x(x^2-3y^2)\right), && (21)
\end{aligned}$$

where,

$$b_1 = a_1\frac{1-C}{1+C} = \frac{4}{\phi\, b}\sin(\frac{\phi}{2})\frac{1-C}{1+C} \quad (22)$$

$$b_2 = a_2 = \frac{2}{\phi\, b^2}\sin(\phi) \quad (23)$$

$$b_3 = a_3\frac{1-C}{1+C} = \frac{4}{3\phi\, b^3}\sin(\frac{3\phi}{2})\frac{1-C}{1+C}. \quad (24)$$

4 First Order Position and the Value of b

To first order in r/b, Equations 20 and 21 give the familiar expression for the position as a function of A and B,

$$x_1 = \frac{1}{b_1}\frac{A-B}{A+B}, \quad (25)$$

where the subscript 1 on x_1 denotes that this is the first order estimate. From bench test measurements we know that $1/b_1 = 26$ mm to an accuracy of a few %. Using this value, Equation 22 can be solved for C,

$$C = \frac{a_1 - b_1}{a_1 + b_1} = 0.11810 \quad (26)$$

We can also write Equation 22 in terms of an effective radius, $b_{\rm eff}$,

$$b_1 = \frac{4}{\phi\, b_{\rm eff}}\sin(\frac{\phi}{2}). \quad (27)$$

Solving this for $b_{\rm eff}$ gives,

$$b_{\rm eff} = b\frac{1+C}{1-C} = 44.37 \text{ mm}. \quad (28)$$

As expected $b_{\rm eff}$ is larger than the physical radius of 35 mm. Using this value of C provides enough information to determine the values of the b coefficients,

$$b_1 = 3.8461 \times 10^{-2} \text{ mm}^{-1} \quad (29)$$

$$b_2 = 6.3030 \times 10^{-4} \text{ mm}^{-2} \quad (30)$$

$$b_3 = 3.3067 \times 10^{-6} \text{ mm}^{-3} \quad (31)$$

$$r_{31} = b3/b1 = 8.5975 \times 10^{-5} \text{ mm}^{-2}. \quad (32)$$

5 Third Order Position

Using Equations 20 and 21 one can obtain an expression for the third order estimate for the position, x_3,

$$\frac{1}{b_1}\frac{A-B}{A+B} = x_3\,\frac{1 + r_{31}(x_3^2 - 3y^2)}{1 + b_2(x_3^2 - y^2)}, \quad (33)$$

where $r_{31} = b_3/b_1$. The left hand side can be identified as the first order position estimate, x_1. If independent knowledge of y is available, this equation can be solved for x_3,

$$\begin{aligned} x_1(1 + a_2(x_3^2 - y^2)) &= x_3(1 + r_{31}(x_3^2 - 3y^2)) & (34) \\ x_1 + x_1 a_2 x_3^2 - x_1 a_2 y^2)) &= x_3 + r_{31} x_3^3 - 3 r_{31} x_3 y^2)) & (35) \end{aligned}$$

$$x_3^3 - \frac{x_1 a_2}{r_{31}} x_3^2 + \frac{(1 - 3 r_{31} y^2)}{r_{31}} x_3 - \frac{x_1(1 - a_2 y^2)}{r_{31}} = 0. \quad (36)$$

This cubic equation can be solved using a library routine such as the CERNLIB routine DRTEQ3. Inside the domain $|x_3| < 22$ mm and $|y| < 22$ mm, the cubic equation always has one real root and two complex roots; the real root is the unique choice for the solution. As either x or y approach b, the cubic equation has three real roots and it is not immediately obvious which is the correct one. However that situation has never occured during extensive simulation of this model.

In order to solve the cubic equation, one requires an independent estimate of y. There are two obvious options for this,

- Use $y = 0$. This is all that can be done when a single BPM is analyzed in isolation, as is done on the front end computers.
- Use the value of y computed from neighboring BPMs and the knowledge of the lattice, as might be done offline.

6 Simulations

The plots in Figure 2 show the results of computations of A and B computed using Equations 18 and 19 along with Equations 1 and 2. The values of the parameters are, $b = 35$ mm, $\phi = 110°$ and $C = 0.11810$. Both plots show the values of A and B as a function of x, for different values of y and for different orders of approximation in equations Equations 1 and 2. From this we can see that going from first to third order of approximation makes a large change but that adding further orders makes only a small change.

The plot in Figure 3 shows the results of the following study. For different values of x and y, A and B were computed to 11^{th} order. These values were used to compute the first order position estimate, Equation 25. The plot shows the difference between the first order x position estimate and the generated x position, as a function of generated x position. This is done for several different values of y. The horizontal axis covers the full region for which the requirements document specifies an accuracy of less than 1 mm. The first order estimate fails the requirement for large values of x. Interestingly, the accuracy at large x is best when y is also large; this is explained by the relative sign in the $(x^2 - y^2)$ the $(x^2 - 3y^2)$ terms in equations 20 and 21.

The procedure was repeated using the ninth or tenth order calculation of A and B. In these trials, the estimated position changed by less than 1 μm, relative to the trial at eleventh order. From this we conclude that the computation of A and B to eleventh order is more than sufficient to study the quality of the position estimators.

The plots in Figure 4 show the results of computing A and B to eleventh order then computing the position to third order, using Equation 36. The upper and lower plots show the same information but with different vertical scales. In order to use this equation, one must supply an estimate for y. When making this plot, the true value of y was used. While this does not represent how the instrument can be used in the field, it does provide a baseline against which different algorithms for y can be benchmarked. This plot shows that if the quality of the y estimate is excellent, then the worst case bias in the x position estimate is less than 250 μm over the full range of interest, $|x| < 15$ mm and $|y| < 15$ mm.

Figure 5 again shows the results of computing A and B to eleventh order then computing the position to third order, using Equation 36. In this case, however, a value of $y = 0$ was used for computing the estimated position, regardless of the value of y used to compute A and B. Both the upper and lower plots show the same information but on different vertical scales. This calculation simulates a procedure that could be implemented on the front end computers. These plots show that, for $|y| < 10$ mm, the the bias in x is less than the requirement of 1 mm for all values of $|x| < 15$ mm. For $|y| > 10$ mm, however, the bias is larger than the requirement.

Figure 6 again shows the bias that results from computing A and B to eleventh order then computing the position to third order, using Equation 36. For the solid lines, Equation 36 was computed using $y = y_{\rm gen} + 1$ mm, where $y_{\rm gen}$ is the generated value of y. For the dashed lines the position was computed using $y = y_{\rm gen} - 1$ mm. This procedure models the sort of resolution in y that might be available offline by using information from neighboring BPMs. The results are excellent: the bias is less than 550 μm over the full range of interest and less than 200 μm for $|y| < 10$ mm.

7 A Test of the Method

This section will use a method developed in Beams-doc-1863 to look for evidence that the third order correction either works or fails. In this method, three measurements are used:

- p_C Proton central orbit: obtained by measuring the proton position just before the helix is opened.
- p_H Proton helix: obtained by measuring the proton position just after the helix is opened.
- $\bar{p}_H$ Anti-proton helix: obtained by measuring the anti-proton position just after the end of end of anti-proton injection.

If everything is working as planned, then

$$p_H - p_C \quad = \quad -(\bar{p}_H - p_C). \tag{37}$$

Beams-doc-1863 did this study using the first order position estimate. In this note we will repeat the study using the third order position estimate and compare it to the first order result. For this study we need do not have knowledge of the orthogonal coordinate so we set $y = 0$ when computing the third order correction.

Figure 7 shows $p_H - p_C$ plotted against $\bar{p}_H - p_C$. The blue points show the first order calculation and the red points show the third order calculation. [1] The two distributions look much the same.

Figure 8 shows the data from Figure 7 projected onto the resolution axis, the dashed line along the main diagonal. To be precise, the quantity plotted is $(p_H - p_C) + (\bar{p}_H - p_C)$. This shows quantitatively that the third order position estimator is not significantly better or worse than the first order one.

Figure 9 is a sanity check on the size of the corrections. Each plot shows the difference between the third order and first order position measurements. As expected the effect is small on the central orbit and large on the helix.

8 Testing the y Dependent Correction - Part 1

Several years ago, Jim Fitzgerald did some calibration measurements on a spare TeV BPM by passing 53 MHz signals down a wire stretched inside the BPM. He measured the signals on each plate for a grid of wire positions. The two files I used were named, BPM TEV PH 53m10dbm 15mod.xls and BPM TEV PH 53m10dbm 20mod.xls.

So far I have not been able to make sense out of these files. The difference over sum equation, with a scale factor or 26 gives positions that are off by a factor of about 2.5, even for small displacements from the center. Bob Webber pointed out that these data are known to be inconsistent with previous data that gave the scale factor of 26. So this project is on hold for now.

9 Testing the y Dependent Correction - Part 2

Mike Syphers suggested a simple way to compute the value of y that can be used Equation 36. He pointed out that many of the BPMs are in FODO cells, where the distance between quads is $L \approx 30$ m, and the focal lengths of the quads are $F = \pm 24$ m. If an x measuring BPM has two neighbors that measure y, then y at the x measuring BPM can be determined as described below.

[1] In this plot 210 of the 236 BPMs are shown; 5 are excluded because they have no anti-proton cables connected; 18 are excluded because the step size at the helix open is too small to reliably calculate the cancellation coefficients and 3 are excluded because they lie very far from the main body of the data.

Let the y position at the x-measuring BPM be y_0, the y position at the next downstream BPM be y_1 and the y position at the next upstream BPM be y_2. Then y_0 is given by,

$$y_0 = \frac{y_1 + y_2}{2 + L/F} \quad (38)$$

$$\approx 0.3(y_1 + y_2) \quad (39)$$

Valeri Lebedev cautioned that this estimate is for the design lattice and that the real lattice has significant currents in the corrector magnets, with the result that the accuracy of this estimate is probably, at best, about 3 mm. Never-the-less I decided to try.

I obtained a list of BPM positions in the design lattice from Beams-doc-876-v1. From this list I identified 172 BPMs which fit the pattern needed to use Equation 39:

- the nearest neighbors measure the orthogonal coordinate,
- the BPM is separated from its two nearest neighbors by 29.734 m.

A few of these BPMs were dropped from the study because, at the x BPM position, the helix opens mostly in the y direction, giving too short a lever arm for the computation of the cancellation coefficients. This left 158 BPMs to be included in this study. For these BPMs the proton and antiproton positions were recomputed using the third order correction, using the y computed by equation 39. Figure 10 shows a repeat of Figure 7 with the additional points added. Including y in the third order correction does not make a significant improvement to this plot.

Figure 11 shows a repeat of Figure 8 with the green points from Figure 10 added. All three methods of estimating the position have about the same resolution.

Figure 12 shows the size of the y correction to the position. Specifically it shows the difference between the two third order position estimates, the one using $y = 0$ and the one using y from the neighboring BPMs. This can be compared to Figure 9. In the comparison we see that including an estimate for y is a small effect compared to making the step from first order to third order.

The conclusion of this section is that adding the y dependent correction does not improve the resolution in Figure 10. Moreover the size of the correction is small. So it seems likely that the source of the resolution is not the order of the approximation. It is something else.

As an aside, I am curious if Figure 13 can be used to estimate the quality of the y estimate. That figure shows y_2 plotted against y_1. It looks to me as if the points want to lie on an ellipse with a major axis at +45 degrees from the x axis. If this is really the predicted shape, then we can probably infer something about the resolution of the y measurement from the thickness of the band.

10 Summary and Conclusions

Provided that the model of the pickup response and the model of coupling are sufficiently accurate, this note shows that the first order x position estimate passes the accuracy requirement of ± 1 mm for small values of x but that it fails the requirement for large values of x. It also shows that the third order estimate for x, using $y = 0$, meets the requirements over most of the parameter space; it fails only at large y. Finally, if y information derived from neighboring BPMs has an accuracy of about ± 1 mm, then the third order x position estimate, meets the accuracy requirements over the full parameter space.

What remains is to understand if this model of the pickup response and coupling are themselves sufficiently accurate. I tried two methods to address this and neither produced a good answer, either yes or no. I tried using the test stand wire data but that data, or my interpretation of it, is very different than expectations. I also tried to compare the the measured sizes of the proton and anti-proton helices. Using the first order position estimate, that data has a resolution of about 0.7 mm. The higher order corrections are small compared to this width and they do not measurably change the resolution, for good or for bad. Any other ideas for testing the accuracy of the model are welcome.

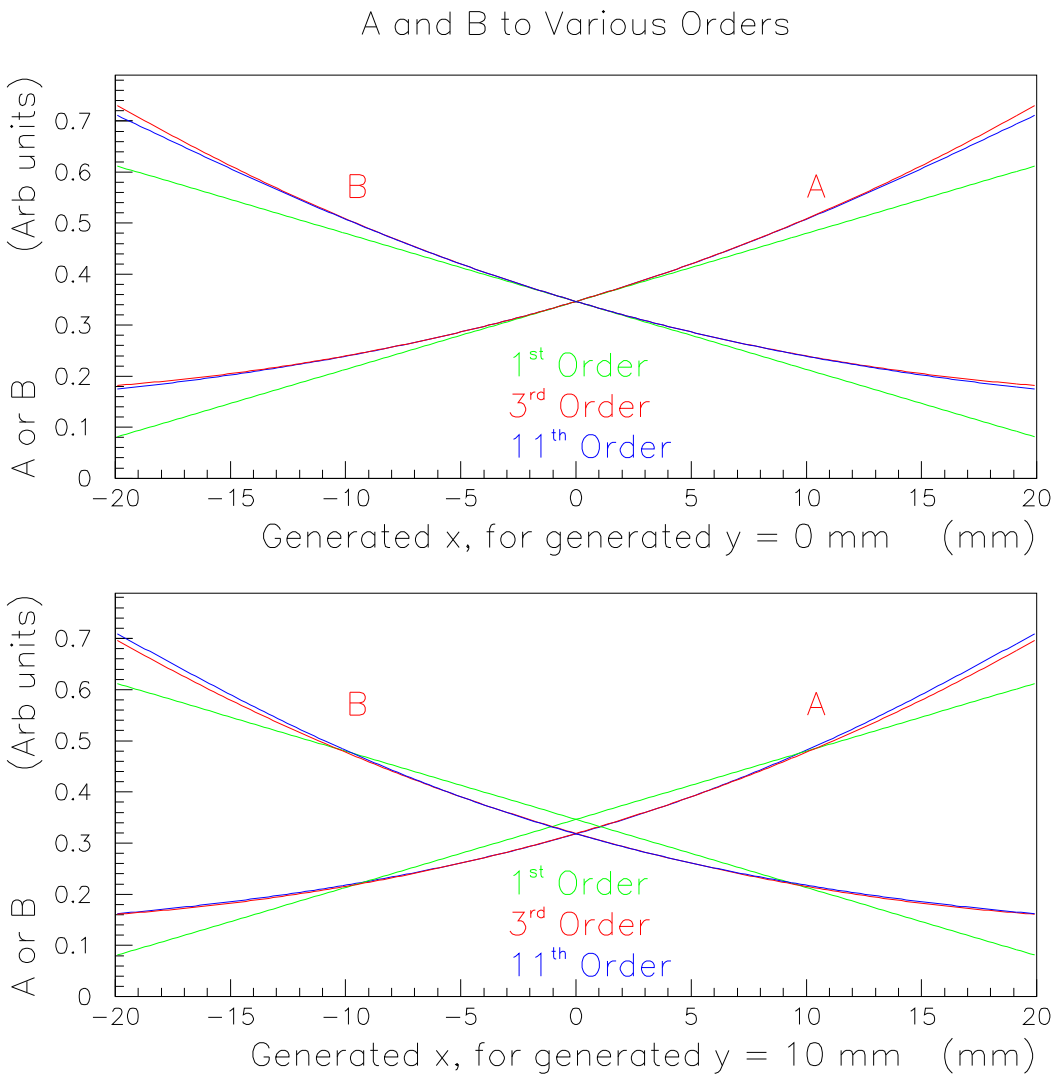

Figure 2: Values for A and B computed using the model described in the text. The upper plot shows A and B as a function of generated x for generated $y = 0$ mm, while the lower plot shows the same quantity for generated $y = 10$ mm. In each case the three lines show different orders of expansion. By 11^{th} order, the expansion has converged at a level corresponding to a position accuracy of better than 1 μm.

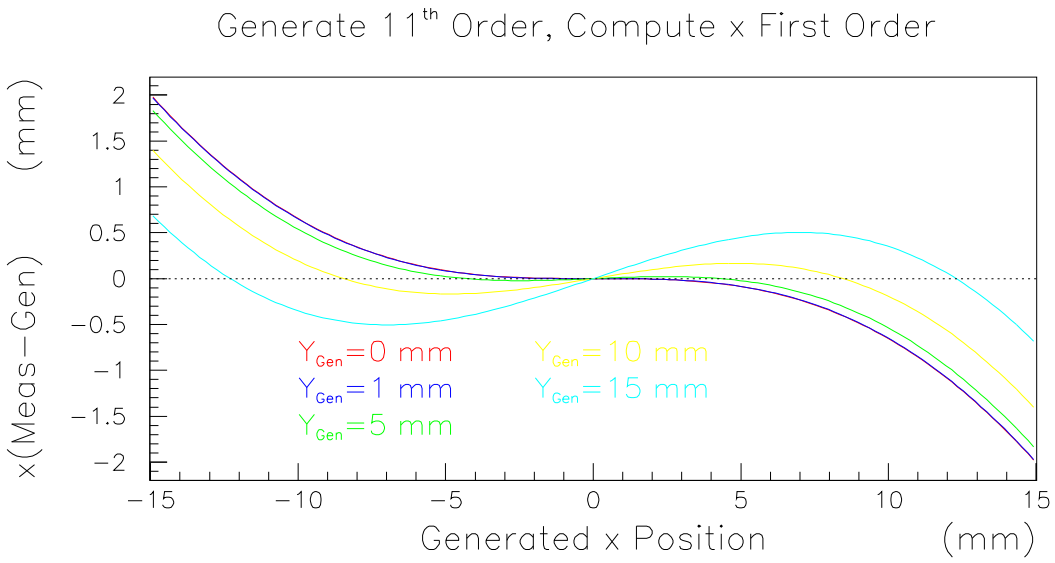

Figure 3: To make this plot A and B were computed to 11^{th} order using the model described in the text. These values were then used to compute the first order x position estimate. The plot shows the bias in the first order x position estimate as a function of the true x position. The different colors correspond to different values of true y position. On this scale the red and blue curves are nearly coincident.

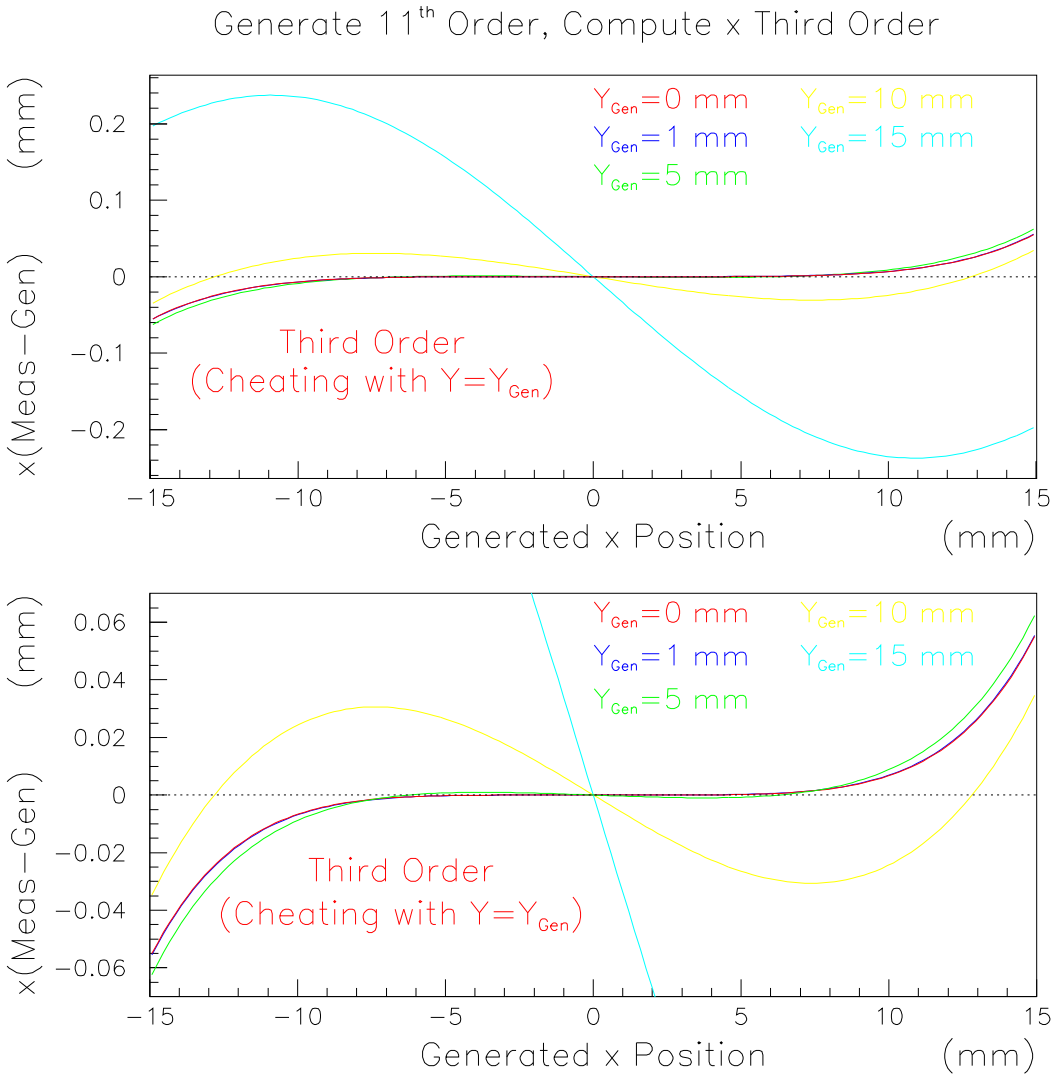

Figure 4: The bias in the third order x position estimate as a function of the true x position. The third order x position estimate was computed with perfect knowledge of the y position. This scenario will not be achieved in the field but it establishes a useful baseline. The different colors correspond to different values of true y position. The upper and lower plots show the same information but on different vertical scales. Even on the expanded vertical scale of the bottom plot, the red and blue curves are nearly coincident.

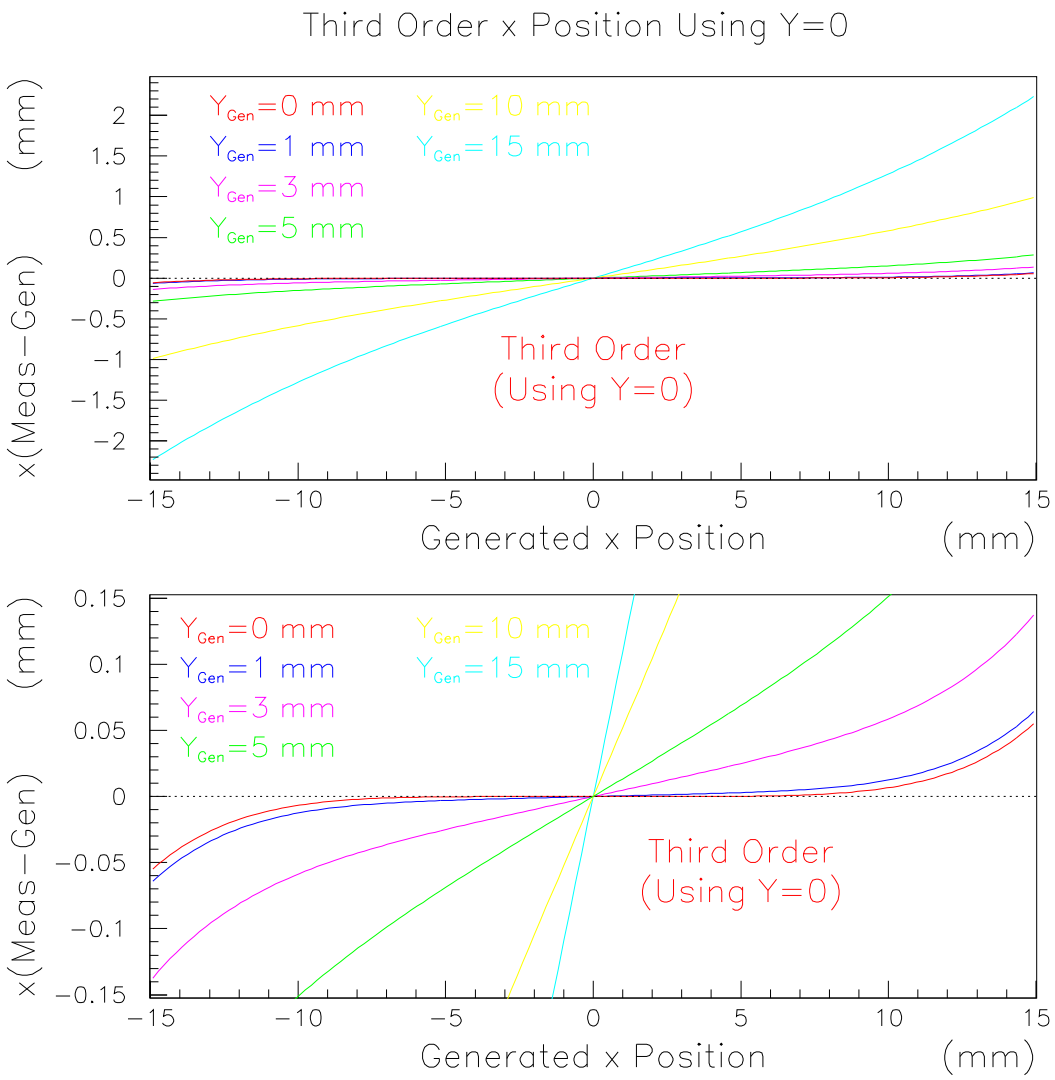

Figure 5: The bias in the third order x position estimate as a function of the true x position. The third order x position estimate was computed using $y = 0$, as can be implemented in the front end computers. The different colors correspond to different values of true y position. The upper and lower plots show the same information but on different vertical scales.

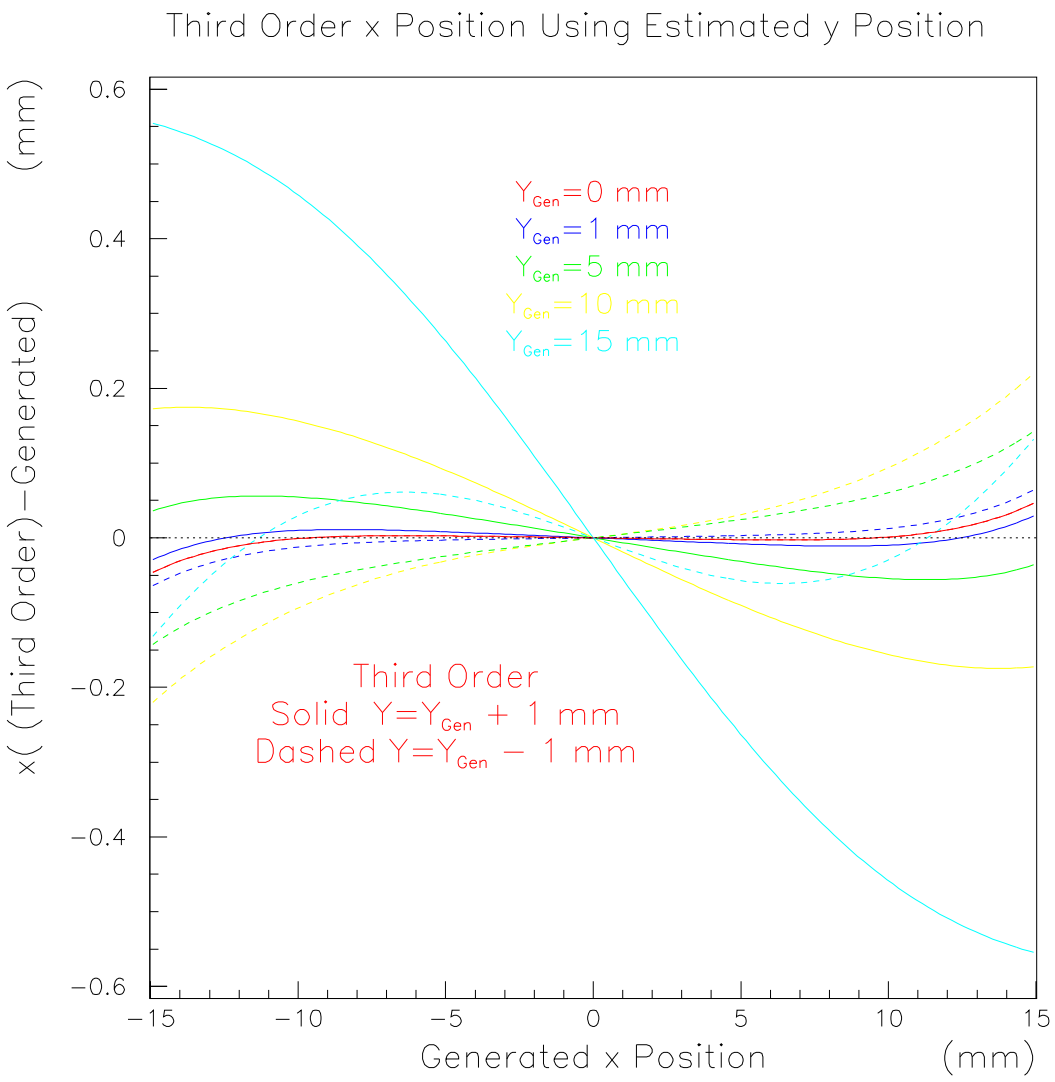

Figure 6: The bias in the third order x position estimate as a function of the true x position. The third order x position estimate was computed using the true value of y plus a bias of $+1$ mm (solid) or -1 mm (dashed). This is intended to estimate the bias in x that might be achieved offline using y information from neighboring BPMs. The different colors correspond to different values of true y position.

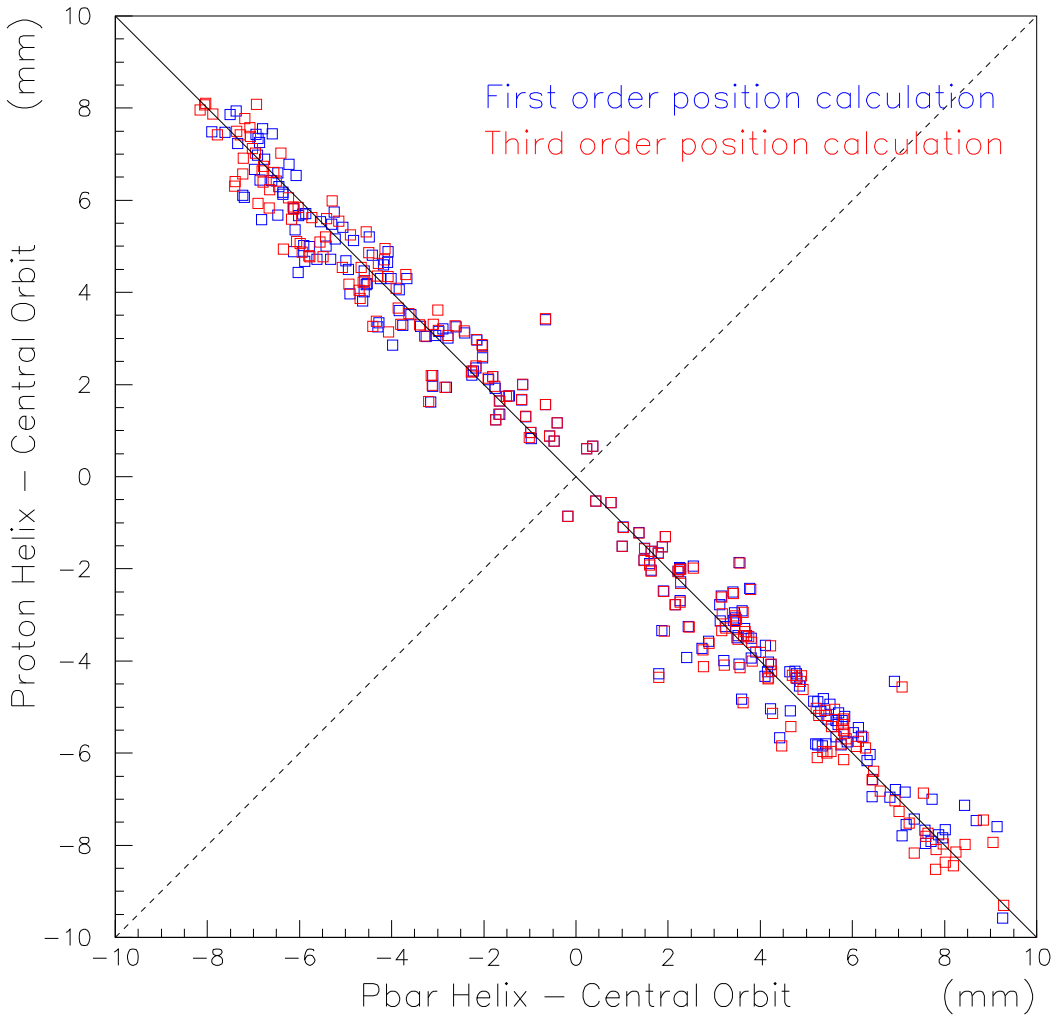

Figure 7: The size of the proton helix ($p_H - p_C$) vs the size of the anti-proton helix ($\bar{p}_H - p_C$), for the first order and third order calculations of the position. The resolution is obtained by projecting the data onto the dashed line along the main diagonal.

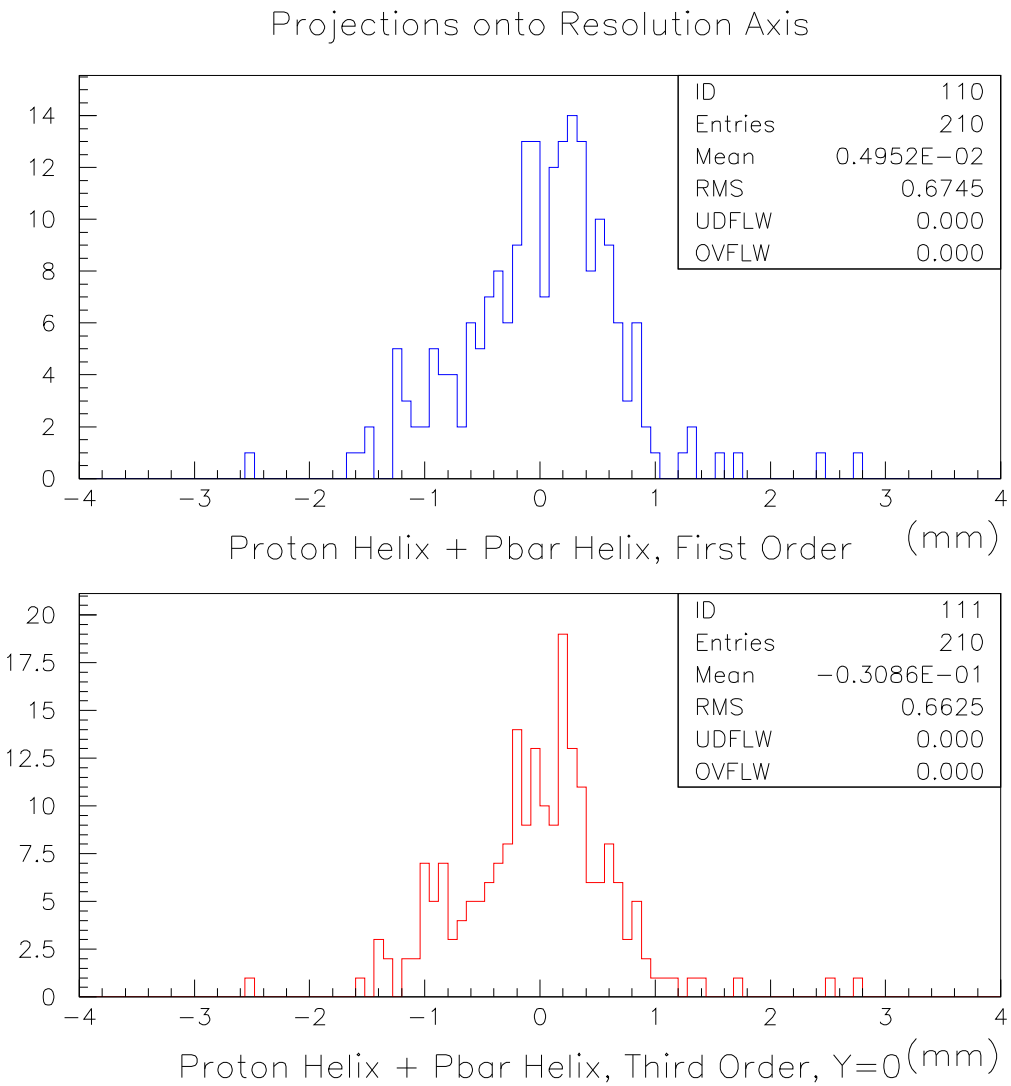

Figure 8: Projections of the data from the previous plot onto the resolution axis. The first and third order calculations have about the same resolution.

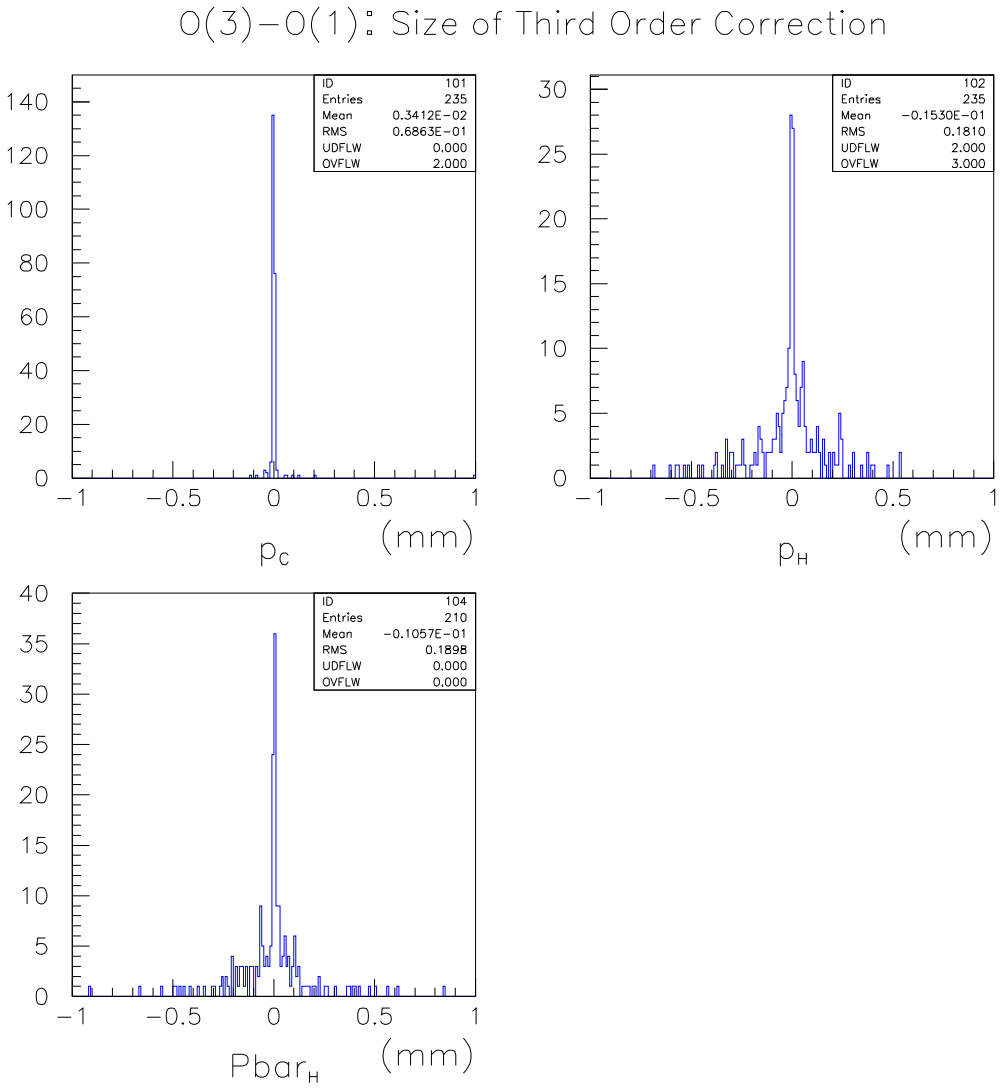

Figure 9: Sanity check on the third order correction. The upper left plot shows the size of the higher order corrections for p_C. The upper right plot shows it for p_H and the lower left for $\bar{p}_H$. As expected the correction is much larger for data with the helix open than for data with the helix closed.

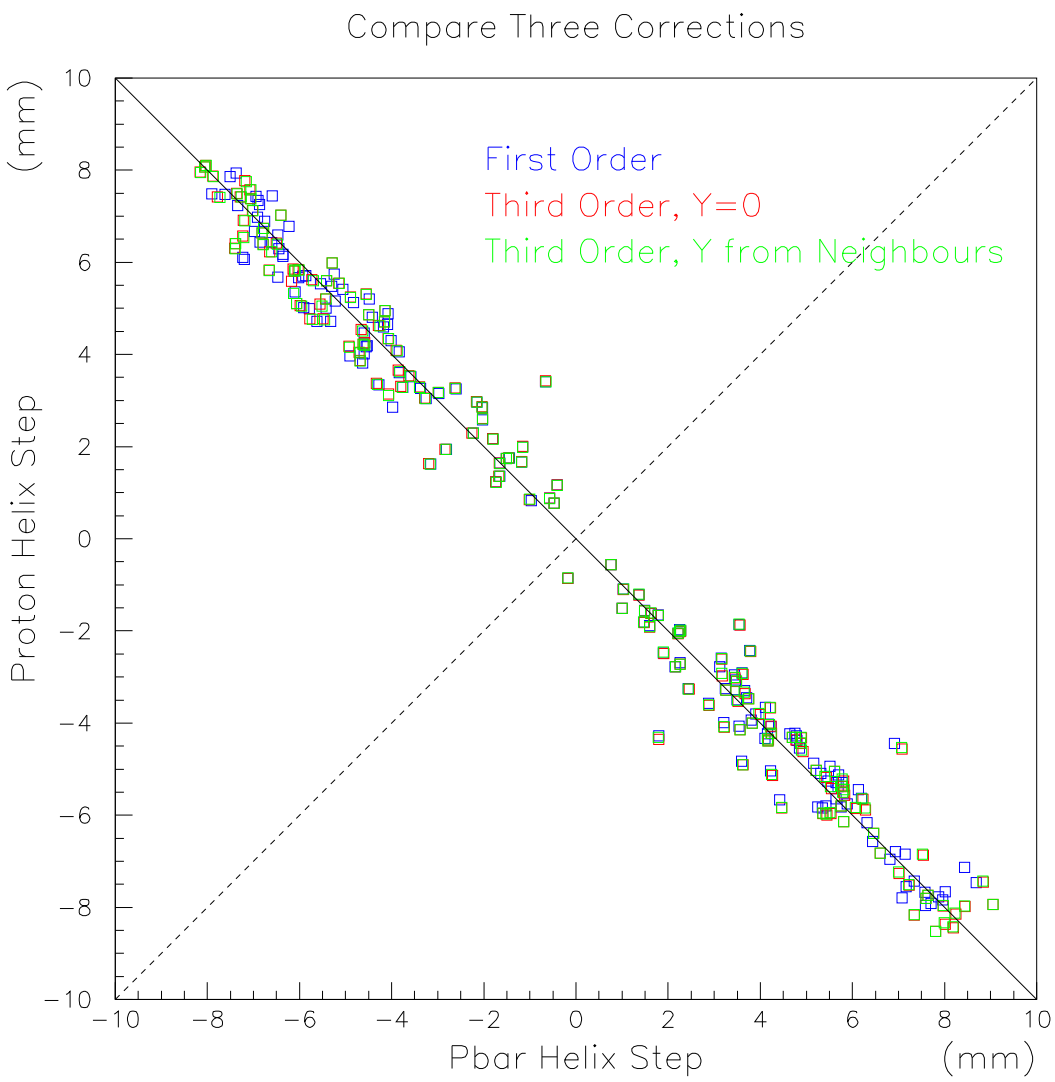

Figure 10: A subset of the data from Figure 7 with the green points added. The green points were computed with the third order correction using y computed from the neighboring BPMs using the simple approximation in equation 39. The subset of data selected is described in detail in the text; in brief it was the subset for which equation 39 is valid.

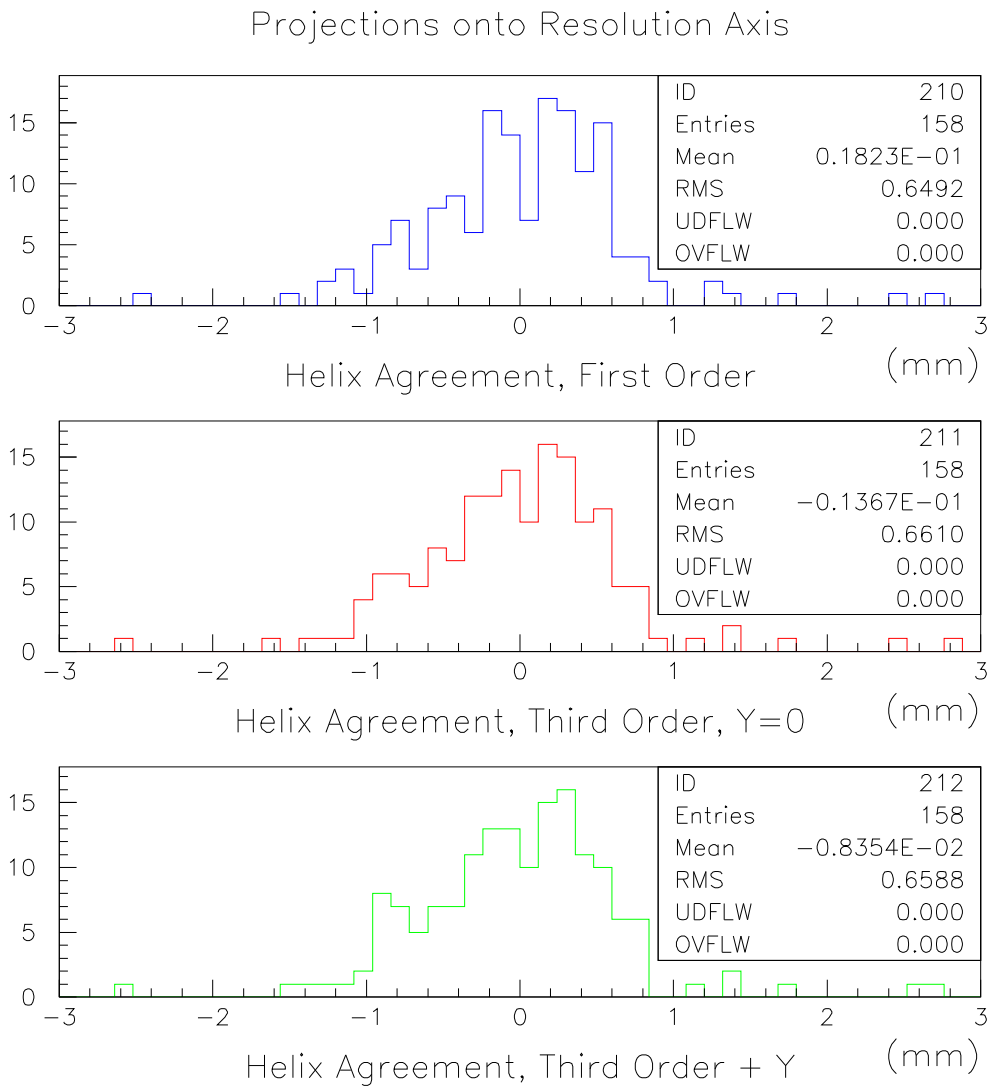

Figure 11: Projections of the previous figure onto the resolution axis. The first two plots on this page are a repeat of Figure 8 but with a few of the data points dropped. All three versions of the position estimate have about the same resolution.

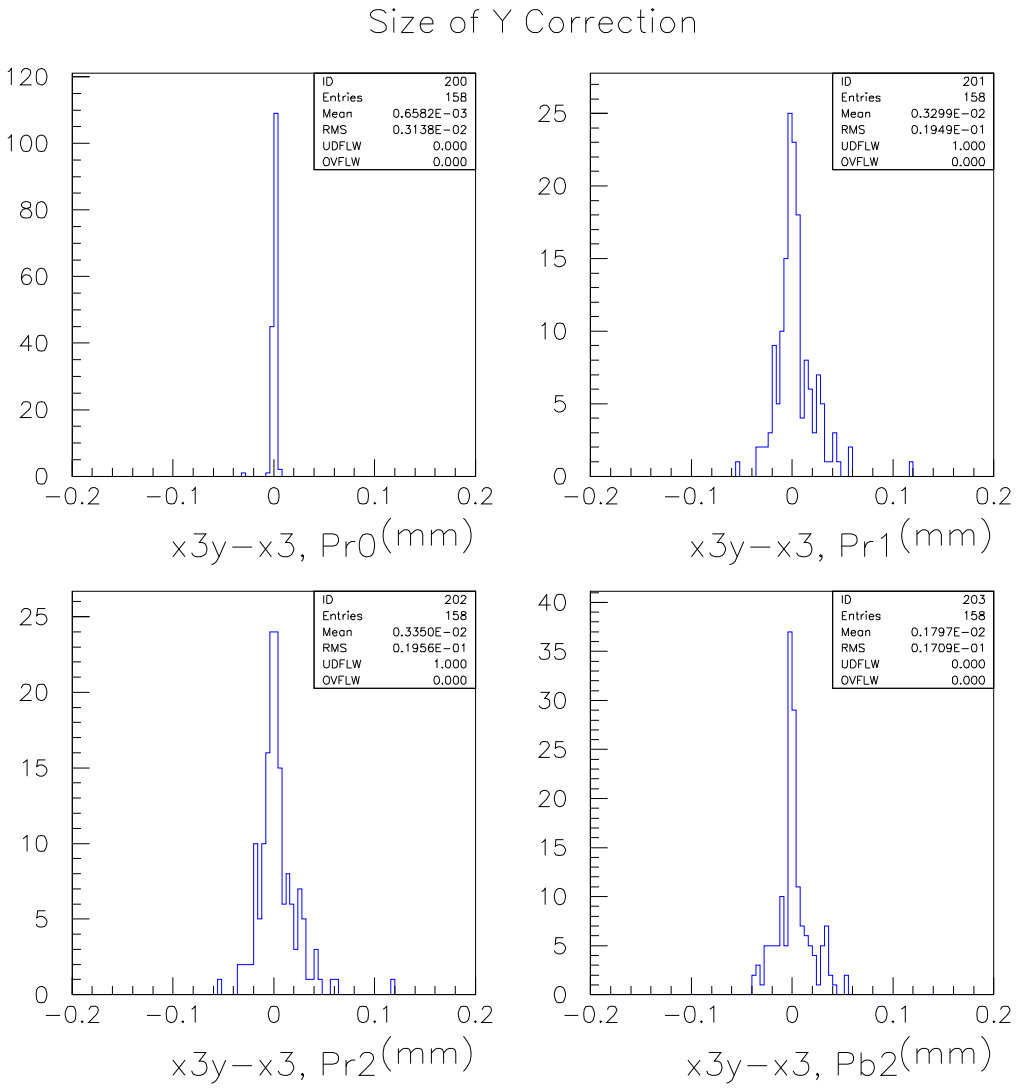

Figure 12: These figures show the difference between the third order position computed using $y = 0$ and the third order position computed using the estimate of y from equation 39. The upper left plot is for protons with the helix closed; the upper right plot is for protons, just after the helix is opened; the lower left plot is for protons, just after the end of antiproton injection; the lower right plot is for anti-protons, just after the end of antiproton injection. As expected the correction is small when the helix is closed and larger when it is opened.

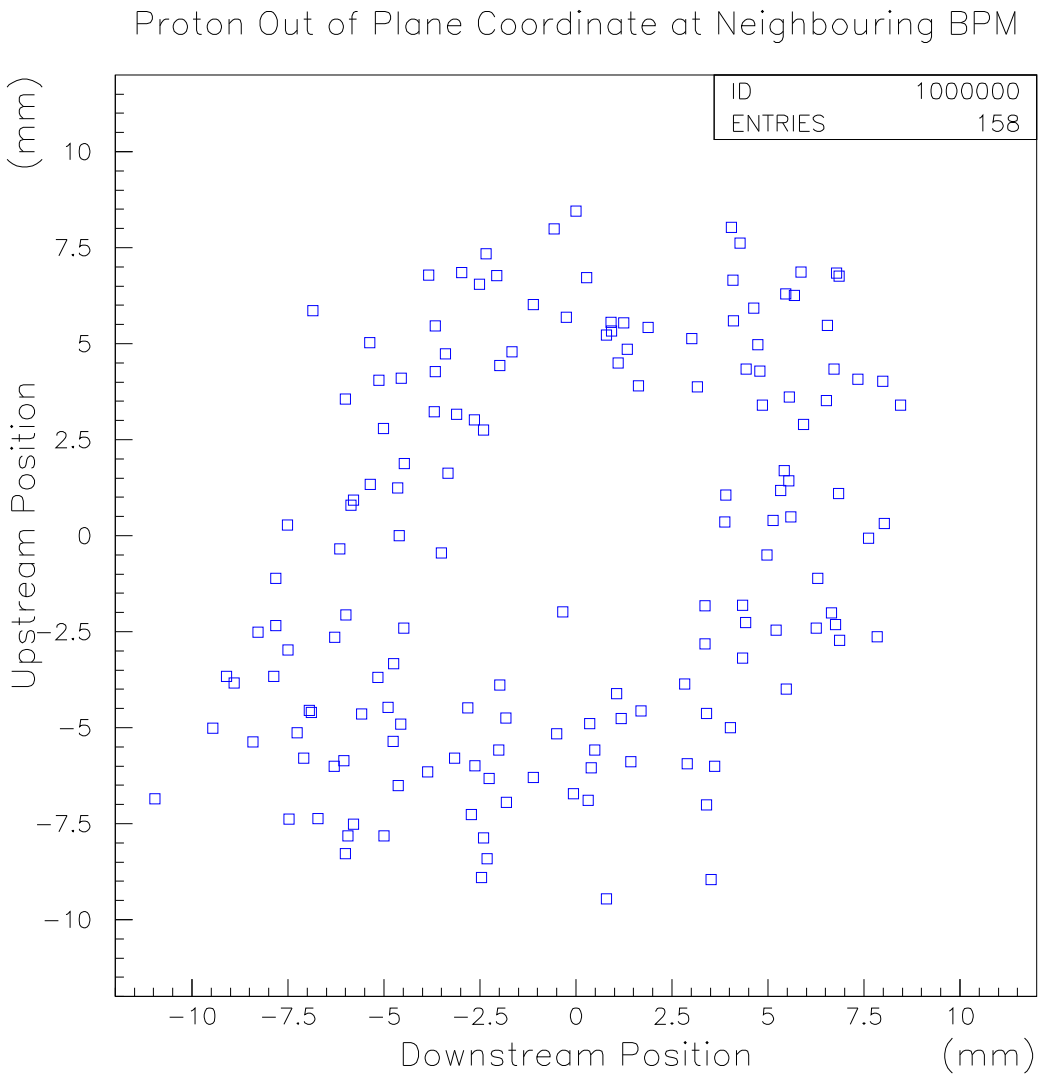

Figure 13: For the BPMs used in this plot, the neighboring BPMs, 29.734 m upstream and downstream, measure y. The plot here shows y_{Upstream} vs $y_{\text{Downstream}}$. I am curious if these data can be used to estimate the resolution on the estimated y position. See the text for details.